Available online at www.sciencedirect.com
ScienceDirect
Bioorganic & Medicinal Chemistry 15 (2007) 2421–2433
Bioorganic & Medicinal Chemistry

Synthesis, pharmacological evaluation and electrochemical studies of novel 6-nitro-3,4-methylenedioxyphenyl-*N*-acylhydrazone derivatives: Discovery of LASSBio-881, a new ligand of cannabinoid receptors

Carolina D. Duarte,[a,b] Jorge L. M. Tributino,[a,c] Daniel I. Lacerda,[a,c] Marina V. Martins,[a,c] Magna S. Alexandre-Moreira,[d] Fernando Dutra,[e] Etelvino J. H. Bechara,[e] Francine S. De-Paula,[f] Marilia O. F. Goulart,[f] Juliano Ferreira,[g] João B. Calixto,[g] Marise P. Nunes,[h] Alvaro L. Bertho,[h] Ana Luisa P. Miranda,[a] Eliezer J. Barreiro[a,b] and Carlos A. M. Fraga[a,b,*]

[a]*LASSBio—Laboratório de Avaliação e Síntese de Substâncias Bioativas, Faculdade de Farmácia, Universidade Federal do Rio de Janeiro, PO Box 68006, 21944-971, Rio de Janeiro, RJ, Brazil*
[b]*Programa de Pós-Graduação em Química Orgânica, Instituto de Química, Universidade Federal do Rio de Janeiro, Rio de Janeiro, RJ, Brazil*
[c]*Departamento de Farmacologia Básica e Clínica, Instituto de Ciências Biomédicas, Universidade Federal do Rio de Janeiro, Rio de Janeiro, RJ, Brazil*
[d]*LaFI—Laboratório de Farmacologia e Imunidade, Departamento de Fisiologia, Centro de Ciências Biológicas, Universidade Federal de Alagoas, Maceió, AL, Brazil*
[e]*Departamento de Bioquímica, Instituto de Química, Universidade de São Paulo, São Paulo, SP, Brazil*
[f]*Instituto de Química e Biotecnologia, Universidade Federal de Alagoas, Maceió, AL, Brazil*
[g]*Departamento de Farmacologia, Centro de Ciências Biológicas, Universidade Federal de Santa Catarina, Florianópolis, SC, Brazil*
[h]*Departamento de Imunologia, Fundação Oswaldo Cruz, Rio de Janeiro, RJ, Brazil*

Received 3 December 2006; accepted 11 January 2007
Available online 17 January 2007

Abstract—We describe herein the discovery of LASSBio-881 (**3c**) as a novel in vivo antinociceptive, anti-inflammatory, and in vitro antiproliferative and antioxidant compound, with a cannabinoid ligand profile. We observed that LASSBio-881 (**3c**) was able to bind to CB1 receptors (71% at 100 μM) and also to inhibit T-cell proliferation (66% at 10 μM) probably by binding to CB2 receptors, in a non-proapoptotic manner, different from anandamide (**1**). It was also demonstrated that LASSBio-881 (**3c**) had an important antioxidant profile toward free radicals (DPPH and hydroxyl), probably due to its particular redox behavior, which reflects the presence of both nitro and 3,5-di-*tert*-butyl-4-hydroxyphenyl sub-units, as demonstrated by cyclic voltammetry studies. In addition, we showed that these structural sub-units are essential for the observed pharmacological activity.
© 2007 Elsevier Ltd. All rights reserved.

1. Introduction

The inflammatory response is a complex set of interactions between cell-derived mediators to attain the recovery of an injured tissue or that could lead to persistent tissue damage by inflammatory cells if assisted repair is not properly achieved.[1] Some of these mediators, for example, eicosanoids, are also able to activate and sensitize nociceptors, leading to hyperalgesic response.[2] The contribution of the eicosanoids to the genesis of several pathological states, such as chronic inflammatory diseases, thrombosis, and pain, is well established.[3] The biosynthesis of such mediators involves a key enzyme, that is, cyclooxygenase (COX).[4] Its constitutive

Keywords: *N*-Acylhydrazone derivatives; Cannabinoid; Analgesic; Anti-inflammatory; Antioxidant activities.
* Corresponding author. Tel.: +55 21 25626503; fax: +55 21 25626644; e-mail: cmfraga@pharma.ufrj.br

0968-0896/$ - see front matter © 2007 Elsevier Ltd. All rights reserved.
doi:10.1016/j.bmc.2007.01.013

isoform, named COX-1, is related to homeostatic functions, such as gastric mucosal cytoprotection, renal blood flow regulation, and vascular antithrombotic activity; while its inducible isoform, COX-2, is overexpressed under stress conditions, although constitutive in a few tissues.[5]

In addition, the role of the endocannabinoid system in the endogenous control of pain[6] and inflammation is widely described in the literature,[7] due to the partial agonism of anandamide (AEA, **1**) (Chart 1) and other endocannabinoids on cannabinoid receptors CB1 and CB2, expressed mainly in brain and immune cells, respectively.[8] Although the activation of brain CB1 receptors leads to undesirable side effects related to Cannabis ingestion, the therapeutic usefulness of CB1 agonists is still valuable in neurotrauma, brain ischemia, pain, and glaucoma. On the other hand, the absence of such psychotropic events on the selective agonism of CB2 receptors has called the attention of medicinal chemists on the development of novel anti-inflammatory and analgesic drugs.[9] The wide chemical diversity of natural and synthetic cannabinoid agonists does not permit the election of a common pharmacophore, since the structure–activity relationships could not be well established.[9]

Other enzymes involved in the inflammatory hyperalgesic response, that is, COX-2 and lipoxygenases, are also able to convert AEA in oxygenated products (prostamides), which can bind to cannabinoid receptors,[10] showing a close connection between these two pathways in a way to control the inflammatory process.

As a consequence of inflammatory response, there is a massive production of reactive oxygen species (ROS), which have been recently recognized as true messengers, and even their toxic effects are viewed as the result of the perversion of an otherwise physiological extra/intracellular signaling.[11] This is crucial in inflammatory disorders in the central nervous system, for example, cerebral ischemia-reperfusion injury, Alzheimer's disease, and pre-senile dementia.[12] Nimesulide (**2**) was recently described as neuroprotective both in vivo and in vitro, and this activity is due to both anti-inflammatory and antioxidant properties.[13]

N-Acylhydrazones (NAH) have been widely described by our group as potent anti-inflammatory, antinociceptive, and anti-platelet compounds,[14] due to their ability to mimic the bis-allylic moiety of unsaturated fatty acids and amides, for example, arachidonic acid (AA), precursor of eicosanoid biosynthesis, and AEA (**1**), involved in the endocannabinoid system.[15] This can be rationalized

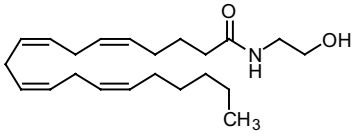

Chart 1.

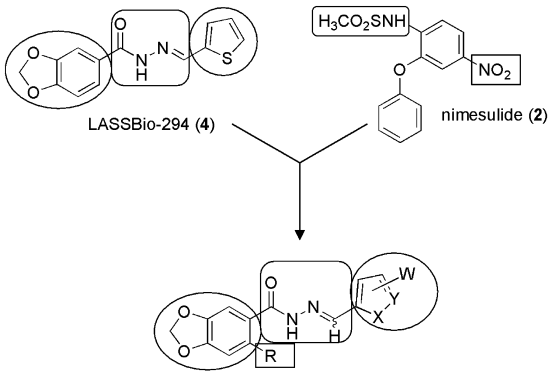

(**3a**) LASSBio-879 - R = NO_2; X = O; Y = CH; W = H
(**3b**) LASSBio-880 - R = NO_2; X = S; Y = CH; W = H
(**3c**) LASSBio-881 - R = NO_2; X = CH=CH; Y = CH; W = 3,5-di*tert*butyl-4-hydroxy
(**3d**) LASSBio-882 - R = NO_2; X = CH=CH; Y = CH; W = H
(**3e**) LASSBio-934 - R = NO_2; X = N; Y = CH=CH; W = H
(**3f**) LASSBio-935 - R = NO_2; X = CH=CH; Y = N; W = H
(**3g**) LASSBio-936 - R = NO_2; X = NH; Y = CH; W = H
(**5**) LASSBio-945 - R = H; X = CH=CH; Y = CH; W = 3,5-di*tert*butyl-4-hydroxy

Scheme 1. Design concept of new 6-nitro-3,4-methylenedioxyphenyl-*N*-acylhydrazone derivatives (**3**).

by the relative acidity of the amide hydrogen of the NAH group as well as its capacity of stabilizing free radicals.[15]

In this context, the aim of our present work was the development of novel drug candidates with an in vivo anti-inflammatory and antinociceptive profile, presenting also an antioxidant activity, based on our previous results concerning the medicinal chemistry of NAH derivatives.[16] The rational approach leading to the new 6-nitro-3,4-methylenedioxyphenyl-*N*-acylhydrazones (**3**) (Scheme 1) includes the molecular hybridization[17] between LASSBio-294 (**4**), a potent analgesic (ID_{50} = 8.1 μmol/kg—abdominal constrictions induced by acetic acid in mice) and anti-platelet derivative (IC_{50} = 15.3 μM—rabbit platelet aggregation induced by AA, inhibiting the production of thromboxane B_2) but poor anti-inflammatory,[18] and nimesulide (**2**), an anti-inflammatory drug with in vivo antioxidant properties,[13] in order to optimize the anti-inflammatory profile of lead-compound (**4**). The nature of the aryl groups attached to the imine sub-unit of compounds (**3**) that are 2-thiophenyl, 2-furyl, 2-pyrrolyl, 2-pyridinyl, 4-pyridinyl, and phenyl was selected based on classical ring isosteric replacement.[17] In addition, we elected the 3,5-di-*tert*-butyl-4-hydroxyphenyl group in an attempt to optimize the radical scavenging potential.[19] We also synthesized compound (**5**) (Scheme 1), to evaluate the possible contribution of the nitro group in the modulation of the redox properties and bioactivity.

2. Results and discussion

2.1. Chemistry

The new substituted 6-nitro-3,4-methylenedioxyphenyl-*N*-acylhydrazone derivatives (**3**) and (**5**) were synthesized from safrole (**6**) (Scheme 2), an abundant natural product from Brazilian flora, the major constituent of

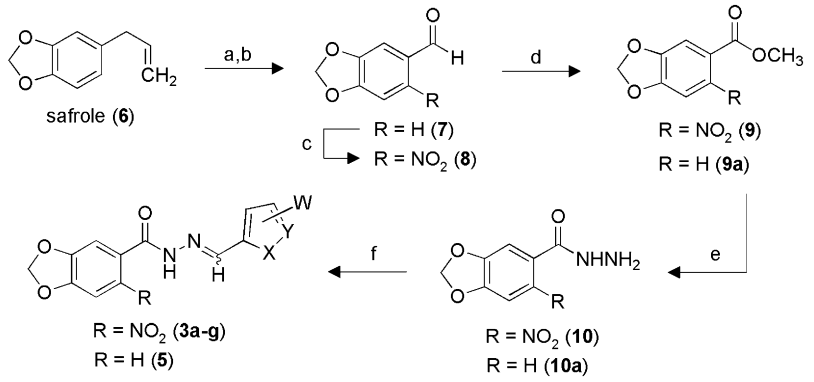

Scheme 2. Synthesis of compounds (**3a**–**g** and **5**). Reagents and conditions: (a) KOHaq 3 N, *n*-BuOH, rt, 3h; (b) i—O_3/O_2, AcOH, 0 °C, 1 h; ii—Zn°, AcOH (75%, three steps); (c) HNO_3, 20–25 °C, 0.5 h, 95%; (d) I_2, KOH, MeOH, 0 °C, 1.5 h, 88%; (e) $N_2H_4{\cdot}H_2O$ 80%, EtOH, ta, 1 h, 70%; (f) ArCHO, EtOH, HCIcat, rt, 0.5 h.

Sassafras oil from *Ocotea pretiosa* and of extracts from *Piper hispidinervum*[20] (Scheme 1). After isomerization and oxidative cleavage,[21] we obtained piperonal (**7**) in 75% yield from (**6**), which was submitted to nitration[22] with concentrated nitric acid at 20–25 °C, and further oxidation[14c] to the corresponding methyl ester (**9**) by treatment of the aldehyde (**8**) with 2.6 equiv of KOH and 1.3 equiv of iodine in methanol at 0 °C, in 94% yield over two steps. Absorption bands at 1509 and 1038 cm^{-1} in the infrared spectrum clearly show the presence of the nitro group; additionally, the presence of two singlets at 7.03 and 7.38 ppm in the aromatic region of the ^1H NMR spectrum characterizes the AB pattern of the aromatic ring. These data, which are in complete agreement with previous results from the literature,[22] demonstrate unequivocally that the nitration occurred regioselectively at the position 6 of the 1,3-benzodioxole ring. The key hydrazide intermediate (**10**) was then obtained in 70% yield, by treating an ethanolic solution of (**9**) with hydrazine hydrate at room

Table 1. New NAH target compounds (**3a**–**g**) and (**5**)

Compound	Substituent	Yield (%)	Melting point (°C)	*E*/*Z* ratio[a]
3a LASSBio-879		88	226–228	60:40
3b LASSBio-880		90	240–242	60:40
3c LASSBio-881	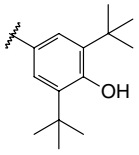	82	280–282	67:33
3d LASSBio-882		95	216–218	70:30
3e LASSBio-934	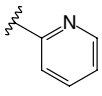	84	184–185	70:30
3f LASSBio-935	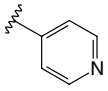	89	202–203	70:30
3g LASSBio-936	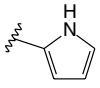	83	212–213	57:43
5 LASSBio-945	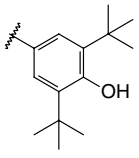	91	231–232	—

[a] Calculated from ^1H NMR iminic hydrogen integration, according to Karabatsos et al.[23]

temperature.[14c] Piperonylhydrazide (**10a**) was also obtained from safrole (**6**), using the same synthetic strategy, as previously described by our group.[14c]

Finally, the new NAH target compounds (**3a**–**g**) and (**5**) (Table 1) were obtained, in 70–95% yield, by acid-catalyzed condensation of (**10**) with the appropriate aromatic aldehydes in ethanol.[14c] Our next step was to determine the relative configuration of the imino double bond in NAH derivatives (**3a**–**g**), in order to assure the diastereomeric ratio. Analysis of the ^{1}H NMR spectra revealed the presence of two singlet signals in an average proportion of 65:35, corresponding to the *E* and *Z* imine-attached hydrogens, respectively (Table 1), due to the stereoelectronic effects of the nitro group *ortho* to the NAH moiety. The assignment of each diastereomer was made in agreement with the previous work of Karabatsos et al.[23] for the relative configuration of hydrazones and related compounds, which describes that the imino hydrogen of the *E*-diastereomer is 0.2–0.3 ppm downfield from the corresponding *Z*-diastereomer.[23] On the other hand, we detected the formation of only one diastereomer of compound (**5**), which corresponds to the *E* configuration, according to previous results with LASSBio-294 (**4**) and analogs.[24]

2.2. Anti-inflammatory and analgesic activities

First, we evaluated the in vivo anti-inflammatory profile of 6-nitro-3,4-methylenedioxyphenyl-*N*-acylhydrazone compounds (**3a**–**g**) in the carrageenan-induced rat paw edema,[25] aiming to select the more promising compounds. The new NAH compounds (**3a**–**g**) and (**5**), nimesulide (**2**) and LASSBio-294 (**4**), used as reference compounds, were administered orally at the dose of 300 μmol/kg. The obtained results are disclosed in Table 2.

LASSBio-881 (**3c**) and LASSBio-945 (**5**), which present 3,5-di-*tert*-butyl-4-hydroxyphenyl group attached to the imine function of the NAH moiety, were able to inhibit significantly the edema formation in 31.7% and 36.4%, respectively, without provoking gastric irritation (data not shown). On the other hand, 2-pyridinyl derivative LASSBio-934 (**3e**) presented a moderate ability to inhibit the edema formation, that is, 22.8%, mimicking the anti-inflammatory profile of prototype LASSBio-294 (**4**).[18]

Thus, LASSBio-881 (**3c**) and LASSBio-945 (**5**) were selected for further evaluation of their anti-inflammatory activity in the phorbol ester (TPA)- and AA-induced murine ear edema assays.[26] The first model is characterized by an important participation of the 5-lipoxygenase (5-LO) pathway products, and COX-2 inhibitors do not have any activity in this assay, although they are able to reduce the AA-induced ear edema. The results depicted in Table 3 show that only LASSBio-881 (**3c**) was able to inhibit in 36% the AA-induced ear edema, however, it is not statistically significant even showing a pharmacologic importance.

LASSBio-881 (**3c**) and LASSBio-945 (**5**) were unable to inhibit either phorbol ester or AA-induced edema, as well as LASSBio-294 (**4**).[18] These results indicate that these compounds do not have an inhibitory effect at the AA-cascade level.

Besides the anti-inflammatory activity of compounds LASSBio-881 (**3c**) and LASSBio-945 (**5**), we have also investigated their antinociceptive profile in the formalin-induced murine hypernociception model[27] (Table 4). This assay elicits a neurogenic phase followed by an inflammatory event. In contrast to nimesulide (**2**), which was able to prevent inflammatory nociception, LASSBio-881 (**3c**) was active in the neurogenic phase, while LASSBio-945 (**5**) and LASSBio-294 (**4**)[18] showed no activity. This central antinociceptive activity was confirmed by the hot plate test in mice,[28] in which only LASSBio-881 (**3c**) was able to increase latency time, indicating an action at central nervous system level (Scheme 3). These results suggest distinct mechanisms of action for compounds LASSBio-881 (**3c**) and LASSBio-945 (**5**).

Table 2. Anti-inflammatory activity of compounds (**3a**–**g**) and (**5**) in carrageenan-induced rat paw edema assay

Compound	Dose (μmol/kg)	*n*[a]	ΔVolume[b] (μL)	Inhibition (%)	ID_{50}(μmol/kg)
Vehicle	—	10	521.8 ± 25.4	—	—
2 Nimesulide	300	5	221.4 ± 42.6	57.5*	22.7
4 LASSBio-294	300	5	366.8 ± 33.3	29.7*	14.3
3a LASSBio-879	300	5	500.1 ± 42.7	4.1 ns[c]	—
3b LASSBio-880	300	5	503.5 ± 44.3	3.4 ns	—
3c LASSBio-881	300	8	356.3 ± 16.0	31.7*	194.7
3d LASSBio-882	300	5	503.1 ± 39.5	3.5 ns	—
3e LASSBio-934	300	8	402.8 ± 40.0	22.8*	—
3f LASSBio-935	300	8	452.4 ± 14.4	13.3 ns	—
3g LASSBio-936	300	8	412.6 ± 22.4	20.9 ns	—
5 LASSBio-945	300	8	331.8 ± 27.6	36.4*	96.5

Compounds were administered orally.
[a] Number of animals.
[b] Results expressed in terms of mean ± SEM.
[c] Not statistically significant.
* $p < 0.05$ (ANOVA One Way followed by Dunnet test).

Table 3. Anti-inflammatory profile of compounds (**3c**) and (**5**) in murine ear edema assay

Compound	Dose (μmol/kg)	TPA-induced murine ear edema			AA-induced murine ear edema		
		n[a]	Edema formation[b] (%)	Inhibition (%)	*n*	Edema formation[c] (%)	Inhibition (%)
Vehicle	—	12	113.9 ± 14.0	—	13	24.5 ± 5.8	—
2 Nimesulide	300	6	126.0 ± 13.4	−10.6 ns[c]	9	−2.3 ± 2.3	100*
4 LASSBio-294	300	6	125.9 ± 19.4	−10.5 ns	10	25.1 ± 5.3	−1.6 ns
3c LASSBio-881	300	6	86.4 ± 8.5	24.1 ns	14	15.8 ± 3.0	36.0 ns
5 LASSBio-945	300	6	136.3 ± 8.4	−19.6 ns	9	18.1 ± 3.3	26.7 ns

Compounds were administered orally.
[a] Number of animals.
[b] Results expressed in terms of mean ± SEM.
[c] Not statistically significant.
* $p < 0.05$ (ANOVA One Way followed by Dunnet test).

Table 4. Antihyperalgesic profile of compounds (**3c**–**d**) and (**5**) in the formalin test

Compound	Dose (μmol/kg)	*n*[a]	1st phase (neurogenic)[b] time (s)	1st phase inhibition (%)	2nd phase (inflammatory)[b] time (s)	2nd phase inhibition (%)
Vehicle	—	10	66.2 ± 5.0	—	169.5 ± 6.0	—
2 Nimesulide	100	7	60.0 ± 2.3	9.3 ns[c]	50.3 ± 2.6	70.3*
4 LASSBio-294	100	10	54.6 ± 4.3	17.9 ns	87.1 ± 9.8	48.6*
3c LASSBio-881	100	8	36.8 ± 1.7	44.5*	146.8 ± 4.0	13.4 ns
3d LASSBio-882	100	6	80.2 ± 6.8	−21.1 ns	167.0 ± 18.5	1.5 ns
5 LASSBio-945	100	8	63.5 ± 3.0	4.1 ns	164.2 ± 2.6	3.1 ns

Compounds were administered orally.
[a] Number of animals.
[b] Results expressed in terms of mean ± SEM.
[c] Not statistically significant.
* $p < 0.05$ (ANOVA One Way followed by Dunnet test).

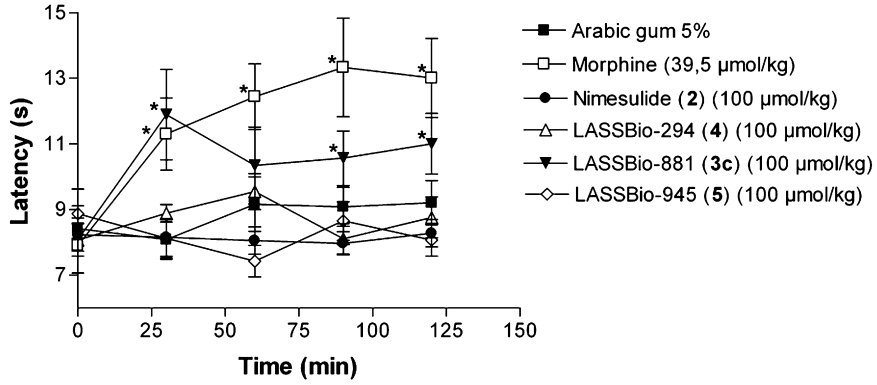

Scheme 3. Time course effect of compounds (**3c**) and (**5**) in the hot plate test. Compounds ere administered orally. Data are expressed as means ± SEM (n = 7–10 animals per group). *$p < 0.05$ (Student's t test) as compared to the vehicle control group.

These results prompted us to evaluate LASSBio-881 (**3c**) on cannabinoid receptors, since its in vivo profile is similar to that previously described for AEA (**1**).[6,7] The in vitro CB1-binding profile was evaluated in murine brain homogenate toward [^{3}H]SR141716A,[29] and results are depicted in Scheme 4. LASSBio-881 (**3c**) was able to displace the radioligand in 71% at 100μM, while LASSBio-945 (**4**) was not able of doing so (ca. 20%), in complete agreement to their in vivo antinociceptive profile. With these results in hands, it can be postulated that LASSBio-881 (**3c**) presented an antinociceptive action probably due to its binding toward CB1-receptors, showing the same profile of AEA (**1**).

We also evaluated the immunomodulatory profile of LASSBio-881 (**3c**) on mitogen (PMA) and anti-CD3 activated spleen T-cells[30] in an attempt to verify the CB2-ligand profile for this compound. Scheme 5 shows that lymphocyte proliferation[31] could be nicely inhibited by LASSBio-881 (**3c**), and this response can be mediated by an action on CB2 receptors, since AEA (**1**) showed the same profile. On the other hand, in contrast to AEA (**1**), LASSBio-881 (**3c**) was not able to induce neither apoptosis nor necrosis[30] (Table 5), showing its specificity in prevention of T-cell proliferation without provoking cell death. These results enable us to rationalize the anti-inflammatory mechanism of LASSBio-881 (**3c**) as an immunomodulatory response, which can be promoted by its action on CB2 receptors.

According to the above-mentioned results, the presence of the nitro group is essential for the central analgesic

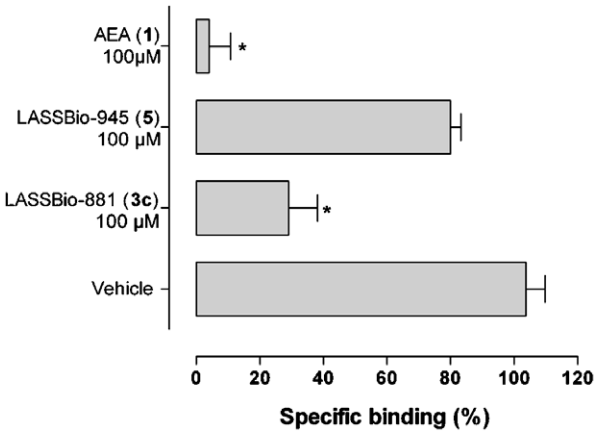

Scheme 4. Effect of compounds (**3c**) and (**5**) in CB1-cannabinoid binding assay. Data are expressed as means ± SEM ($n = 5$ animals per group). $^{*}p < 0.01$ (Student's t test) as compared to the vehicle control group.

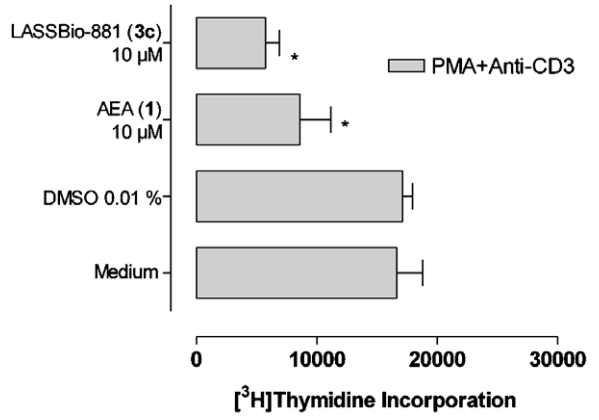

Scheme 5. Inhibition of lymphocyte proliferation by AEA (**1**) and LASSBio-881 (**3c**). Each point represents triplicate determinations and results are based on at least three-independent experiments (means ± SEM). $^{*}p < 0.01$ (Student's t test) as compared to the vehicle control group.

Table 5. Induction of T-lymphocyte apoptosis by AEA but not for LASSBio-881 (**3c**)

Treatment	% Necrosis (7-AAD)	% Apoptosis (Anexine V)
Control	0.3	42
Anti-CD3	0.1	39
Anti-CD3 + AEA (**1**) 10 μM	0.1	50.8*
Anti-CD3 + LASSBio-881 (**3c**) 10 μM	0.0	43.8

Each point represents triplicate determinations and results are based on at least three independent experiments (mean ± SEM).
* $p < 0.01$ (Student's t test) as compared to the test group (anti-CD3).

activity, giving to compound LASSBio-881 (**3c**) the ability to exert both anti-inflammatory and antinociceptive activities, as well as the ability to bind to CB1 receptor. In contrast, it seems that the anti-inflammatory profile is due to the presence of 3,5-di-*tert*-butyl-4-hydroxyphenyl sub-unit, once compound LASSBio-945 (**5**) presents only an anti-inflammatory profile and LASSBio-882 (**3d**) was not anti-edematogenic.

2.3. Electrochemical studies

In order to clarify the relative contributions of the nitro and 3,5-di-*tert*-butyl-4-hydroxyphenyl groups to the redox character, the voltammetric response of LASSBio-881 (**3c**), as well as of LASSBio-945 (**5**) and LASSBio-882 (**3d**), was determined in aprotic media (DMF + TBAP 0.1 M) using a glassy carbon working electrode, Pt and Ag|AgCl, Cl^- 0.1 M, as auxiliary and reference electrode, respectively.[32] Table 6 shows both cathodic and anodic peak potentials for the first reduction ($E\mathrm{pc_I}$) and oxidation ($E\mathrm{pa_I}$) steps, respectively, at a sweep rate of 0.1 V/s.

In electrochemical terms, LASSBio-881 (**3c**) bears mixed electroactivity, due to the presence of the reducible nitroaromatic function, together with the oxidizable hindered phenol, both groups interconnected by a NAH chain. A comparison of LASSBio-881 (**3c**) with LASSBio-882 (**3d**), devoid of the phenol function, and with LASSBio-945 (**5**), a non-nitrated NAH, could explain the influence of each group on the behavior of this class of compounds. The data displayed in Table 6 show that LASSBio-881 (**3c**) exhibits a more complex redox profile, displaying peaks in both cathodic and anodic regions. As seen for LASSBio-945 (**5**) ($E\mathrm{pc_1} = -2.07$ V), NAH sub-unit is also an electroreducible group,[33] however its contribution to reduction potential of both LASSBio-881 (**3c**) ($E\mathrm{pc_1} = -1.02$ V) and LASSBio-882 (**3d**) ($E\mathrm{pc_1} = -1.10$ V) is supplanted by the presence of nitro group, which is more easily reduced. When we compare the $E\mathrm{pc_1}$ values of LASSBio-881 (**3c**) and LASSBio-882 (**3d**), related to the reduction of the nitroaromatic group, it is evident that the electrodonating phenol group impairs the nitroreduction ($\Delta E\mathrm{pc_1} = 0.08$ V), thus reflecting the interaction between both groups through the NAH moiety. Similar effect is observed in the anodic region, where the peaks ($E\mathrm{pa_1}$) for LASSBio-881 (**3c**), LASSBio-945 (**5**), and LASSBio-882 (**3d**) appear at +1.04, +0.84, and +1.35 V, respectively. The anodic waves are related to the oxidation of phenol, in LASSBio-881 (**3c**) and LASSBio-945 (**5**), with a $\Delta E\mathrm{pc_1} = 0.20$ V, the first one being oxidized less easily due to the presence of the electron-withdrawing nitro group. It is not surprising that the electrochemical processes which involve addition or removal of electrons from an organic framework should correlate with the ability of substituents to withdraw or supply electron density to that framework.

2.4. Antioxidant activity

First, we evaluated the in vitro antioxidant profile of compound LASSBio-881 (**3c**) using the 2,2-diphenyl-1-picrylhydrazyl (DPPH) assay,[34] which measures the hydrogen-donating ability of antioxidants to convert stable DPPH free radical to 1,1-diphenyl-2-picrylhydrazine. The reaction is accompanied by a change in color from deep-violet to light-yellow and is monitored spectrophotometrically. BHT (*tert*-butylhydroxytoluene) was used

Table 6. Redox potentials and antioxidant activity of compounds (**3c–d**) and (**5**) on DPPH, hydroxyl radical, and superoxide degradation assays

Compound	Peak potentials		DPPH assay			Hydroxyl radical degradation			Superoxide degradation		
	Epc_1 (V)	Epa_1 (V)	Concentration (mM)	Abs	Scavenging (%)	Concentration (mM)	[TBARS] (μM)[a]	Degradation (%)	Concentration (mM)	Rate (ΔA/min)	Degradation (%)
Vehicle	—	—	—	1.082	—	—	6.459 ± 0.087	—	—	0.0301	—
BHT	—	—	0.1	0.163	84.9*	0.5	0.896 ± 0.043	86.1*	nd	nd	nd
3c LASSBio-881	−1.10	+1.04	0.1	0.736	32.0*	0.5	0.997 ± 0.085	84.6*	0.25	0.0310	−2.9 ns
3d LASSBio-882	−1.02	+1.35	0.1	1.001	7.49 ns[b]	0.5	1.083 ± 0.013	83.2*	0.25	0.0242	19.6 ns
5 LASSBio-945	−2.07	+0.84	0.1	0.628	45.7*	0.5	0.954 ± 0.062	85.2*	nd	nd	nd

[a] Results expressed in terms of mean ± standard deviation.
[b] Not statistically significant.
* $p < 0.01$ (ANOVA One Way followed by Dunnet test).

as reference antioxidant and results are disclosed in Table 6. LASSBio-881 (**3c**) and LASSBio-945 (**5**) showed a scavenging activity of 32.0% and 45.7%, respectively, at 100 μM concentration, due to the 3,5-di-*tert*-butyl-4-hydroxyphenyl moiety, while LASSBio-882 (**3d**), presenting a phenyl sub-unit, was not active (7.5% ns). Thus, the donation of –OH hydrogen of 3,5-di-*tert*-butyl-4-hydroxyphenyl sub-unit is imperatively more effective in terms of antioxidant profile than –NH hydrogen of NAH, in complete agreement with the results obtained from cyclic voltammetric studies, that is, the lesser positive Epa_1, the higher antioxidant activity.

Intending to verify the scavenging effect of LASSBio-881 (**3c**) over reactive oxygen species, we performed the hydroxyl-mediated 2′-deoxyribose degradation assay[35] and tested its effects on superoxide radical production by the xanthine/xanthine oxidase system[36] (Table 6). Compound LASSBio-881 (**3c**) was able to inhibit deoxyribose oxidation by 84.6%, measured as thiobarbituric acid reactive species (TBARS), therefore comparable with the antioxidant effect exerted by all other compounds studied here and the reference compound BHT. Apparently there is no distinguishable effect of the 3,5-di-*tert*-butyl-4-hydroxyphenyl sub-unit, suggesting an important role of the NAH group in the stabilization of radicals, as previously described.[15b] On the other hand, the xanthine/xanthine oxidase-generated superoxide flux remained unchanged, indicating low reactivity of LASSBio-881 (**3c**) and all other compounds with superoxide radical anion.

2.5. Molecular modeling studies

In order to rationalize the molecular mechanism of radical stabilization for LASSBio-881 (**3c**), molecular modeling studies were performed, using semiempirical AM1 method[37] available in the Spartan 1.0.5 Pro software.[38] According to the results from the synthesis of LASSBio-881 (**3c**) described above, we obtained a mixture of *E* and *Z*-diastereomers, in an approximate 65:35 ratio, measured by NMR.[23] In the present study, we considered both diastereomers and the relative stabilities of corresponding low energy conformers are shown in Table 7.

It is clear that the *syn-E* is the most stable conformer of LASSBio-881 (**3c**). This result corroborates the experimentally obtained NMR-determined diastereomeric ratio, showing major formation of the *E*-diastereomer. We have noticed the possibility of intramolecular hydrogen bonding between the amidic hydrogen and one of the oxygen atoms from nitro group in both diastereomers in all conformers. Consequently, it was also found that the NAH chain is not planar in relation to the 1,3-benzodioxolyl system, that is, dihedral angle between C6═C5–C1′═O of ca. 100°, as a result of an *ortho* effect of nitro group as well as hydrogen bonding between amidic N–H and the nitro group, with the formation of a 7-membered ring shape.

With the minimum energy conformers of both *E*- and *Z*-diastereomers in hands, we followed the studies focusing

Table 7. Conformers from systematic conformational analysis for LASSBio-881 (**3c**)

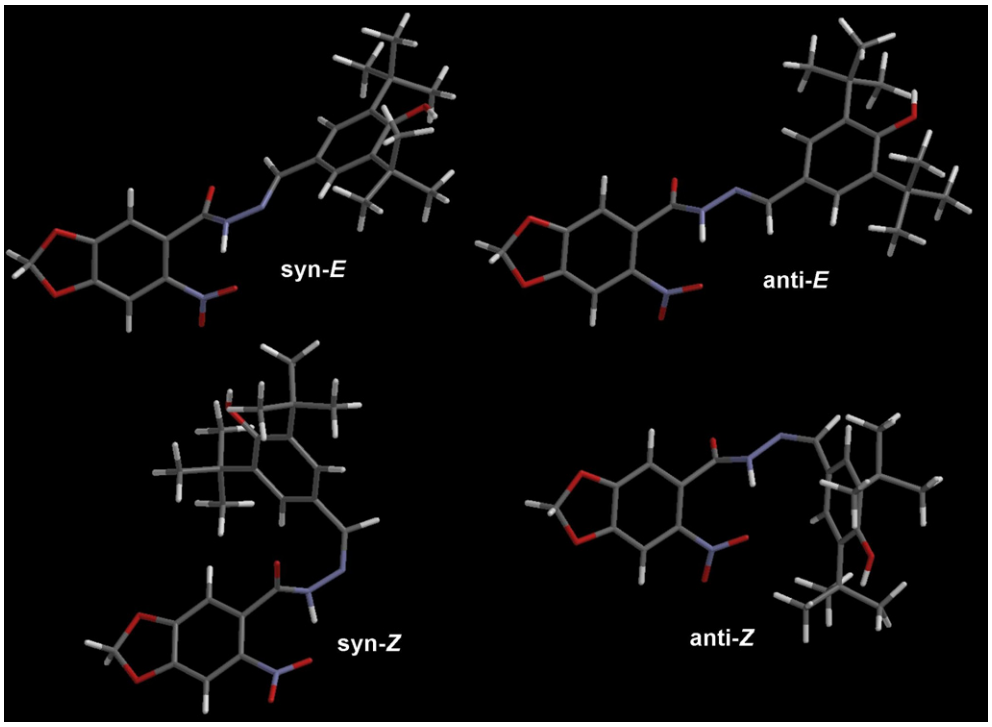

Conformer	AM1 ΔH_f (kcal/mol)	Relative stability $\Delta\Delta H_f$ (kcal/mol)	C6=C5–C1′=O dihedral angle (°)	N–H···$^-$O–N=O distance (Å)
syn-E	−67.39	0.00	98.7	2.56
anti-E	−62.94	4.45	102.3	2.32
syn-Z	−65.18	2.21	96.7	2.37
anti-Z	−66.89	0.50	98.7	2.43

on the stability of radicals of LASSBio-881 (**3c**). This compound, as evidenced in the electrochemical studies, has a dual behavior with the ability of accepting electrons in the nitro group and donating hydrogen atoms from either amidic N–H or phenolic O–H. Considering these three possibilities of radical formation, we analyzed their relative stability, as well as their heats of formation from the corresponding singlet neutral starting diastereomers. In addition, we have analyzed the single occupied molecular orbital (SOMO) energies (Table 8).

According to these results, the radical anion formation is energetically favored, as it is an exothermic process ($\Delta\Delta H_f \sim -53$ kcal/mol) when comparing to *N*-($\Delta\Delta H_f \sim +32$ kcal/mol) and *O*-radical ($\Delta\Delta H_f \sim +36$ kcal/mol). The energies of SOMO also reveal that the nitro group, which is able to work as electron acceptor in single electron transfer (SET) processes,[39] has a critical role in radical formation from neutral LASSBio-881 (**3c**). Concerning the donation of radical hydrogen (H$^\bullet$) from either amide NAH or phenol hydroxyl subunits, we can consider these functional groups as energetically equivalent electron donors, being the corresponding radical species formed endothermically. Their corresponding SOMO energy values also show the same pattern of donating behavior for both

Table 8. Energy profile of radicals generated from neutral LASSBio-881 (**3c**)

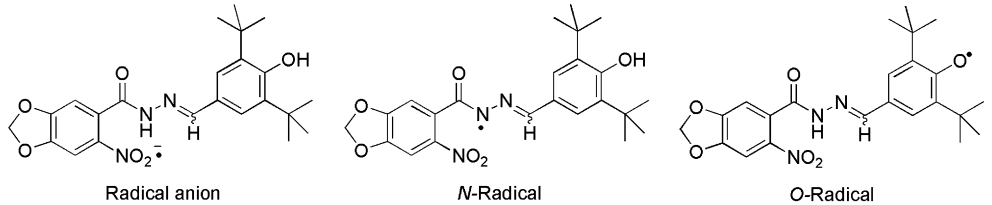

Conformer	AM1 ΔH_f neutral (kcal/mol)	AM1 ΔH_f radical anion (kcal/mol)	E_{SOMO} radical anion (eV)	AM1 ΔH_f *N*-radical (kcal/mol)	E_{SOMO} *N*-radical (eV)	AM1 ΔH_f *O*-radical (kcal/mol)	E_{SOMO} *O*-radical (eV)
syn-E	−67.39	−120.00	−2.98	−35.20	−1.80	−31.10	−1.68
anti-Z	−66.89	−120.18	−2.90	−33.48	−1.62	−29.42	−1.67

groups, which can be an attribute of resonance stabilizing effect.

3. Conclusions

LASSBio-881 (**3c**) was identified as a novel central antinociceptive and peripheral anti-inflammatory compound, acting probably as a non-selective cannabinoid ligand, in a different manner from its lead compounds LASSBio-294 (**4**) and nimesulide (**2**). In addition, we observed that LASSBio-881 (**3c**) was able to bind to CB1 receptors and also to inhibit T-cell proliferation probably through the binding of CB2 receptors, in a non-proapoptotic manner, different from AEA (**1**).

It was also demonstrated that LASSBio-881 (**3c**) exhibited important antioxidant properties probably due to its particular redox profile, which reflects its structural features by the presence of both nitroaryl and 3,5-di-*tert*-butyl-4-hydroxyphenyl sub-units.

In addition, we showed that these sub-units are also essential for the pharmacological activity. We observed the importance of the nitro group of LASSBio-881 (**3c**) for the antinociceptive activity, as well as for the CB1-binding profile, since LASSBio-945 (**5**) was inactive. Otherwise, the anti-inflammatory activity of LASSBio-881 (**3c**) is probably due to its 3,5-di-*tert*-butyl-4-hydroxyphenyl radical scavenging sub-unit, considering that LASSBio-945 (**5**) presented only an anti-inflammatory activity and LASSBio-882 (**3d**) did not present anti-edematogenic properties.

4. Experimental

4.1. Chemistry

Reactions were routinely monitored by thin-layer chromatography (TLC) in silica gel (F245 Merck plates) and the products visualized with iodine or ultraviolet lamp (254 and 365 nm). ^{1}H and ^{13}C nuclear magnetic resonance (NMR) spectra were determined in DMSO-d_6 solutions using a Bruker AC-200 spectrometer. Peak positions are given in parts per million (δ) from tetramethylsilane as internal standard, and coupling constant values (J) are given in Hertz. Infrared (IR) spectra were obtained using a Nicolet Magna IR 760 spectrometer. Samples were examined as potassium bromide (KBr) disks. Melting points were determined using a Quimis instrument and are uncorrected. Column chromatography purifications were performed using silica gel Merck 230–400 mesh. All described products showed ^{1}H and ^{13}C NMR spectra according to the assigned structures. All organic solutions were dried over anhydrous sodium sulfate and all organic solvents were removed under reduced pressure in rotatory evaporator.

4.1.1. 6-Nitro-1,3-benzodioxole-5-carbaldehyde (8).[22] A mixture of 1 g (6.7 mmol) of tritured piperonal (**7**) and 3.3 mL of concentrated nitric acid was kept at 20–25 °C, in a water bath, observing complete dissolution of starting material. After 30 min, addition of distilled water provoked the crystallization of a light yellow solid, which was filtered and washed with 200 mL of distilled water and recrystallized from ethanol/water (1.24 g, 95%); mp 91–92 °C (lit. 93–94 °C[21]). ^{1}H NMR (200 MHz, DMSO-d_6, TMS) δ (ppm): 6.34 (s, 2H, H-2); 7.32 (s, 1H, H-4); 7.74 (s, 1H, H-7); 10.09 (s, 1H, –C*H*O). RMN ^{13}C (50 MHz, DMSO-d_6, TMS) δ (ppm): 104.8 (C-2); 105.4 (C-7); 107.4 (C-4); 127.9 (C-5); 146.1 (C-6); 151.8 (C-3); 152.3 (C-1); 188.6 (C=O). IR (ε_{max}, KBr) ε (cm^{-1}): 1682, 1518, 1368, 1336, 1126, 1119, 1032, 1021.

4.1.2. Methyl 6-nitro-1,3-benzodioxole-5-carboxylate (9).[14c] To a solution of (**8**) (1.5 g, 7.7 mmol) in absolute methanol (10 mL) cooled at 0°C were successively added methanolic solutions (each 10 mL) of iodine (2.54 g, 23.1 mmol) and KOH (1.3 g, 23.1 mmol) at 0 °C. After stirring for 1.5 h at 0 °C, small amounts of saturated $NaHSO_3$ solution were added until the disappearance of the brown color. Next, the methanol was almost totally evaporated under reduced pressure. To the residue was added water, and the desired product (**9**) was obtained by filtration and recrystallized in ethanol/water as a light yellow solid (1.52 g; 88%); mp 102-103 °C. ^{1}H NMR (200 MHz, $CDCl_3$, TMS) δ (ppm): 3.89 (s, 3H, OCH_3); 6.18 (s, 2H, H-7); 7.03 (s, 1H, H-4); 7.38 (s, 1H, H-2). ^{13}C NMR (50 MHz, $CDCl_3$, TMS) δ (ppm): 53.5 (O*C*H$_3$); 103.8 (C-2); 105.1 (C-7); 108.6 (C-4); 124.0 (C-5); 143.2 (C-6); 149.8 (C-3); 151.5 (C-1); 165.9 (C=O). IR (ε_{max}, KBr) ε (cm^{-1}): 1717, 1509, 1488, 1362, 1272, 1108, 1038.

4.1.3. 6-Nitro-1,3-benzodioxole-5-carbohydrazide (10).[14c] To a solution of 0.5 g (2.22 mmol) of (**9**) in 2 mL of ethanol was added 6.7 mL of 80% hydrazine monohydrate. The reaction mixture was kept in ambient temperature for 2 h, when TLC indicated the end of the reaction. Then, the media were neutralized with concentrated HCl in an ice bath and the resulting precipitate was filtered out and recrystallized from ethanol–water, affording the title compound as a yellow solid (0.35 g, 70%), mp 184–185 °C. RMN ^{1}H (200 MHz, DMSO-d_6, TMS) δ (ppm): 4.42 (s, 2H, NH_2); 6.26 (s, 2H, H-2); 7.03 (s, 1H, H-4); 7.64 (s, 1H, H-7); 9.59 (s, 1H, N*H*). RMN ^{13}C (50 MHz, DMSO-d_6, TMS) δ (ppm): 104.2 (C-2); 105.3 (C-7); 108.5 (C-4); 128.3 (C-5); 141.9 (C-6); 148.8 (C-3); 151.7 (C-1); 165.2 (C=O). IR (ε_{max}, KBr) ε (cm^{-1}): 3336, 3199, 3120, 1670, 1519, 1502, 1475, 1328, 1257, 1030, 880.

4.1.4. General procedure for preparation of 6-nitro-*N*′-arylmethylidene-1,3-benzodioxole-5-carbohydrazines (3) and (5).[14c] To a solution of 1 mmol of (**10**) or (**10a**) in absolute ethanol (10 mL) containing two drops of 37% hydrochloric acid was added 1 mmol of corresponding aromatic aldehyde derivative. The mixture was stirred at room temperature for 30 min, then after extensive precipitation, was visualized. Next, the mixture was poured into cold water, neutralized with 10% aqueous sodium bicarbonate solution, and the precipitate formed was filtered out and recrystallized from ethanol–water.

4.1.5. *N*′-(2-Furylmethylidene)-6-nitro-1,3-benzodioxole-5-carbohydrazine (3a). The derivative (**3a**) was obtained as a yellow solid by condensation of (**10**) with furfuraldehyde (0.26 g; 88%), mp 226–228 °C. ^{1}H NMR (200 MHz, DMSO-d_6, TMS) δ (ppm): 6.30 (s, 10H, H-2*E*/*Z*); 6.54 (dd, 2H, J = 1.8 Hz, H-4″*Z*); 6.64 (dd, 3H, J = 1.8 Hz, H-4″*E*); 6.72 (d, 2H, J = 3.4 Hz, H-3″*Z*); 6.95 (d, 3H, J = 3.4 Hz, H-3″*E*); 7.15 (s, 2H, H-4′*Z*); 7.30 (s, 3H, H-4′*E*); 7.74 (d, 7H, J = 4.6 Hz, H-5″*Z*, H-4*E*/*Z*); 7.87 (d, 5H, H-5″*E*, H-7*Z*); 8.10 (s, 3H, H-7*E*); 11.87 (s, 2H, H-2′*Z*); 11.90 (s, 3H, H-2′*E*). ^{13}C NMR (50 MHz, DMSO-d_6, TMS) δ (ppm): 104.4 (C-2); 104.7 (C-7); 105.5 (C-4); 108.5 (C-3″); 108.9 (C-3″); 112.5 (C-4″); 112.7 (C-4″); 128.6 (C-5); 134.9 (C-4′); 138.1 (C-4′); 141.2 (C-6); 145.5 (C-5″); 145.9 (C-5″); 148.8 (C-2″); 149.6 (C-2″); 152.2 (C-1a); 152.6 (C-3a); 161.9 (C-1′); 167.9 (C-1′). IR (ε_{max}, KBr) ε (cm^{-1}): 3197, 3123, 3061, 2918, 2855, 1644, 1623, 1533, 1504, 1486, 1381, 1293, 1281, 1261, 1164, 1126, 1033, 1017, 939, 877, 763.

4.1.6. 6-Nitro-*N*′-(2-thienylmethylidene)-1,3-benzodioxole-5-carbohydrazine (3b). The derivative (**3b**) was obtained as a yellow solid by condensation of (**10**) with 2-thiophenecarboxaldehyde (0.29 g; 90%), mp 240–242 °C. ^{1}H NMR (200 MHz, DMSO-d_6, TMS) δ (ppm): 6.30 (s, 10H, H-2*E*/*Z*); 7.03 (dd, 2H, J = 3.6 Hz, H-4″*Z*); 7.13 (m, 5H, H-4″*E*, H-3″*Z*); 7.31 (m, 5H, H-3″*E*, H-4′*Z*); 7.50 (m, 5H, H-4′*E*, H-5″*Z*); 7.71 (m, 8H, H-4*E*/*Z*, H-5″*E*); 8.14 (s, 2H, H-7*Z*); 8.42 (s, 3H, H-7*E*); 11.88 (s, 2H, H-2′*Z*); 11.92 (s, 3H, H-2′*E*). ^{13}C NMR (50 MHz, DMSO-d_6, TMS) δ (ppm): 104.4 (C-7); 104.5 (C-2); 105.4 (C-4); 108.6 (C-5″); 108.9 (C-5″); 128.1 (C-5); 128.2 (C-4″); 128.3 (C-4″); 129.1 (C-3″); 129.7 (C-3″); 130.9 (C-4′); 131.8 (C-4′); 141.5 (C-6); 143.4 (C-5″); 148.7 (C-1a); 149.1 (C-3a); 152.2 (C-2″); 152.6 (C-2″); 161.7 (C-1′); 167.8 (C-1′). IR (ε_{max}, KBr) ε (cm^{-1}): 3191, 3073, 3060, 3032, 2992, 2915, 2844, 1639, 1608, 1591,1560, 1531, 1503, 1485, 1380, 1290, 1264, 1222, 1162, 1125, 1033, 1015, 928, 878, 713.

4.1.7. *N*′-(3,5-Di-*tert*-butyl-4-hydroxybenzylidene)-6-nitro-1,3-benzodioxole-5-carbohydrazine (3c). The derivative (**3c**) was obtained as a yellow solid by condensation of (**10**) with 3,5-di-*tert*-butyl-4-hydroxybenzaldehyde (0.36 g; 82%), mp 280–282 °C. ^{1}H NMR (200 MHz, DMSO-d_6, TMS) δ (ppm): 1.32 (s, 18H, –CH_3*Z*); 1.40 (s, 36H, –CH_3*E*); 6.29 (m, 6H, H-2*E*/*Z*); 7.15 (m, 6H, H-2″,6″*E*/*Z*); 7.27 (s, 1H, H-4*Z*); 7.47 (s, 2H, H-4*E*); 7.67 (m, 1H, H-4′*Z*); 7.73 (s, 2H, H-4′*E*); 7.83 (s, 3H, H-7*E*/*Z*); 11.69 (s, 1H, H-2′*Z*); 11.76 (s, 2H, H-2′*E*). ^{13}C NMR (50 MHz, DMSO-d_6, TMS) δ (ppm): 30.5 (–*C*H$_3$); 34.9 (*C*-Me$_3$); 104.0 (C-7); 104.2 (C-2); 108.7 (C-4); 124.0 (C-5); 124.4 (C-2″,6″); 128.6 (C-1″); 139.5 (C-3″,5″); 142.0 (C-6); 145.0 (C-4′); 148.6 (C-4″); 152.5 (C-1a); 156.3 (C-3a); 167.7 (C-1′). IR (ε_{max}, KBr) ε (cm^{-1}): 3593, 3172, 3065, 2962, 2872, 1662, 1612, 1527, 1509, 1487, 1433, 1401, 1372, 1342, 1259, 1236, 1212, 1139, 1117, 1032, 927, 875, 766.

4.1.8. *N*′-Benzylidene-6-nitro-1,3-benzodioxole-5-carbohydrazine (3d). The derivative (**3d**) was obtained as a yellow solid by condensation of (**10**) with benzaldehyde (0.30 g; 95%), mp 216–218 °C. ^{1}H NMR (200 MHz, DMSO-d_6, TMS) δ (ppm): 6.31 (s, 66H, H-2*E*/*Z*); 7.34 (m, 165H, H-2″,3″,4″,5″,6″*E*/*Z*); 7.45 (s, 10H, H-4*Z*); 7.72 (s, 23H, H-4*E*); 7.76 (s, 33H, H-7*E*/*Z*); 7.99 (s, 10H, H-4′*Z*); 8.22 (s, 23H, H-4′*E*); 11.94 (s, 10H, H-2′*Z*); 11.97 (s, 23H, H-2′*E*). ^{13}C NMR (50 MHz, DMSO-d_6, TMS) δ (ppm): 104.4 (C-2); 104.6 (C-7); 108.6 (C-4); 108.9 (C-4); 127.1 (C-3″,5″); 127.7 (C-3″,5″); 128.4 (C-5); 129.2 (C-2″,6″); 129.3 (C-2″,6″); 130.4 (C-4″); 130.7 (C-4″); 141.6 (C-6); 144.8 (C-4′); 148.8 (C-4′); 152.3 (C-1a); 152.7 (C-3a); 162.0 (C-1′); 168.0 (C-1′). IR (ε_{max}, KBr) ε (cm^{-1}): 3222, 3114, 3059, 2916, 2851, 1646, 1607, 1533, 1503, 1485, 1381, 1279, 1161, 1123, 1033, 928, 878, 768, 693.

4.1.9. 6-Nitro-*N*′-(2-pyridinylmetilidene)-1,3-benzodioxole-5-carbohydrazine (3e). The derivative (**3e**) was obtained as a yellow solid by condensation of (**10**) with 2-pyridinecarboxaldehyde (0.26 g; 84%), mp 184–185 °C. ^{1}H NMR (200 MHz, DMSO-d_6, TMS) δ (ppm): 6.32 (s, 20H, H-2*E*/*Z*); 7.37 (m, 10H, H-5″,6″*E*/*Z*); 7.58 (s, 10H, H-4*E*/*Z*); 7.74 (m, 10H, H-7*E*/*Z*); 7.91 (m, 10H, H-4″*E*/*Z*); 8.03 (s, 3H, H-4′*Z*); 8.24 (s, 7H, H-4′*E*); 8.54 (d, 3H, J = 3.6 Hz, H-3″*Z*); 8.62 (d, 7H, J = 4.2 Hz, H-3″*E*); 12.15 (s, 3H, H-2′*Z*); 12.19 (s, 7H, H-2′*E*). ^{13}C NMR (50 MHz, DMSO-d_6, TMS) δ (ppm): 104.5 (C-2); 104.6 (C-7); 105.5 (C-4); 108.7 (C-3″); 108.9 (C-3″); 119.5 (C-5″); 120.5 (C-5″); 124.8 (C-4″); 125.1 (C-4″); 127.2 (C-5); 137.3 (C-4′); 137.4 (C-4′); 144.8 (C-6); 150.0 (C-6″); 150.1 (C-6″); 153.2 (C-1a); 155.5 (C-3a); 155.9 (C-2″); 156.2 (C-2″); 165.4 (C-1′); 171.3 (C-1′). IR (ε_{max}, KBr) ε (cm^{-1}): 3427, 3198, 3122, 3063, 2983, 2925, 2854, 1663, 1609, 1523, 1505, 1485, 1432, 1368, 1336, 1288, 1262, 1163, 1126, 1032, 921, 874, 777, 762, 640, 583.

4.1.10. 6-Nitro-*N*′-(4-pyridinylmetilidene)-1,3-benzodioxole-5-carbohydrazine (3f). The derivative (**3f**) was obtained as a yellow solid by condensation of (**10**) with 4-pyridinecarboxaldehyde (0.28 g; 89%), mp 202–203 °C. ^{1}H NMR (200 MHz, DMSO-d_6, TMS) δ (ppm): 6.31 (s, 20H, H-2*E*/*Z*); 7.32 (d, 6H, J = 4.9 Hz, H-2″,6″*Z*); 7.52 (s, 3H, H-4*Z*); 7.71 (d, 14H, J = 5.8 Hz, H-2″,6″*E*); 7.77 (s, 7H, H-4*E*); 7.99 (s, 3H, H-4′*Z*); 8.23 (s, 7H, H-4′*E*); 8.56 (d, 6H, J = 4.9 Hz, H-3″,5″*Z*); 8.68 (d, 14H, J = 5.8 Hz, H-3″,5″*E*); 12.27 (s, 3H, H-2′*Z*); 12.30 (s, 7H, H-2′*E*). ^{13}C NMR (50 MHz, DMSO-d_6, TMS) δ (ppm): 104.7 (C-2,7); 108.6 (C-4); 121.2 (C-3″,5″); 121.7 (C-3″,5″); 124.9 (C-5); 141.7 (C-6); 142.2 (C-4′); 144.7 (C-4″); 145.0 (C-4″); 145.8 (C-4′); 150.2 (C-2″,6″); 150.3 (C-2″,6″); 152.5 (C-1a); 153.4 (C-3a); 167.0 (C-1′); 171.5 (C-1′). IR (ε_{max}, KBr) ε (cm^{-1}): 3450, 3198, 3119, 3050, 2996, 2920, 2857, 1670, 1581, 1530, 1508, 1489, 1421, 1370, 1337, 1298, 1268, 1162, 1125, 1030, 923, 881, 818, 744, 693, 537.

4.1.11. 6-Nitro-*N*′-(1H-pyrrol-2-ylmethylidene)-1,3-benzodioxole-5-carbohydrazine (3g). The derivative (**3g**) was obtained as a yellow solid by condensation of (**10**) with 1H-pyrrol-2-ylcarboxaldehyde (0.27 g; 89%), mp 202–203 °C. ^{1}H NMR (200 MHz, DMSO-d_6, TMS) δ

(ppm): 6.06 (d, 3H, $J = 2.8$ Hz, H-4″*Z*); 6.14 (d, 4H, $J = 2.6$ Hz, H-4″*E*); 6.29 (s, 17H, H-2*E*/*Z*,3″*Z*); 6.47 (s, 4H, H-3″*E*); 6.82 (s, 3H, H-5″*Z*); 6.93 (s, 4H, H-5″*E*); 7.11 (s, 3H, H-4′*Z*); 7.27 (s, 4H, H-4′*E*); 7.70 (s, 3H, H-4*Z*); 7.72 (s, 4H, H-4*E*); 7.86 (s, 3H, H-7*Z*); 8.07 (s, 4H, H-7*E*); 10.83 (s, 3H, H-1″*Z*); 11.54 (s, 4H, H-1″*E*); 11.60 (s, 3H, H-2′*Z*); 11.62 (s, 4H, H-2′*E*). ^{13}C NMR (50 MHz, DMSO-d_6, TMS) δ (ppm): 104.4 (C-4″); 104.8 (C-4″); 105.4 (C-2); 108.5 (C-7); 108.9 (C-4); 109.8 (C-3″); 109.9 (C-3″); 112.1 (C-5″); 112.9 (C-5″); 117.3 (C-5); 122.5 (C-5″); 123.3 (C-5″); 131.7 (C-2″); 132.2 (C-2″); 137.8 (C-4′); 141.0 (C-4′); 144.9 (C-6); 151.6 (C-1a); 155.3 (C-3a); 164.6 (C-1′); 170.6 (C-1′). IR (ε_{max}, KBr) ε (cm^{-1}): 3478, 3412, 3190, 3113, 3054, 2914, 2855, 1638, 1604, 1536, 1502, 1484, 1427, 1384, 1333, 1298, 1263, 1164, 1127, 1035, 928, 874, 744, 551.

4.1.12. *N*′-(3,5-Di-*tert*-butyl-4-hydroxybenzylidene)-1,3-benzodioxole-5-carbohydrazine (5). The derivative (**5**) was obtained as a white solid by condensation of (**10a**) with 3,5-di-*tert*-butyl-4-hydroxybenzaldehyde (0.36 g; 91%), mp 231–232 °C. ^{1}H NMR (200 MHz, DMSO-d_6, TMS) δ (ppm): 1.33 (s, 18H, –CH_3); 5.41 (s, 1H, –OH); 6.22 (s, 2H, H-2); 6,92 (dd, 1H, $J = 8.2$ Hz, 0.4 Hz, H-7); 7.15 (s, 2H, H-2″,6″); 7.37 (dd, 1H, $J = 1.7$ Hz, 0.4 Hz, H-4); 7.51 (dd, 1H, $J = 8.2$ Hz, 1.7 Hz, H-6); 8.06 (s, 1H, H-4′); 11.87 (s, 1H, H-2′). ^{13}C NMR (50 MHz, DMSO-d_6, TMS) δ (ppm): 30.7 (–*C*H$_3$); 35.0 (*C*-Me$_3$); 102.3 (C-2); 108.0 (C-4); 108.6 (C-7); 123.2 (C-6); 124.4 (C-2″,6″); 126.2 (C-1″); 127.9 (C-5); 139.7 (C-3″,5″); 147.9 (C-4′); 149.5 (C-4″); 150.5 (C-3a); 156.6 (C-1a); 162.5 (C-1′).

4.2. Pharmacology

4.2.1. Carragenaan-induced rat paw edema assay.[25] Fasted Wistar rats of both sexes (150–200 g) were used. Compounds were administered orally (300 μmol/kg; 0.1 mL/20 g) as a suspension in 5% arabic gum in saline (vehicle). Control animals received an equal volume of vehicle. One hour later, the animals were injected with either 0.1 mL of 1% carrageenan solution in saline (0.1 mg/paw) or sterile saline (NaCl 0.9%), into the subplantar surface of one of the hind paws, respectively. The paw volumes were measured 3 h after the subplantar injection using a glass plethysmometer coupled to a peristaltic pump. The edema was calculated as the volume variation between the carrageenan- and saline-treated paw. Nimesulide (300 μmol/kg) was used as standard drug in the same conditions. Anti-inflammatory activity was expressed as % of inhibition of the edema when compared with the vehicle control group.

4.2.2. AA- and TPA-induced murine ear edema.[26] Ear edema was induced by administration of arachidonic acid (AA—500 μg/ear) or 12-*O*-tetra-decanoylphorbol 13-acetate (TPA—2 μg/ear) in fasted Swiss mice weighing 28–25 g. AA and TPA were dissolved in acetone and 20 μl of solution was applied to the inner and outer surface of the right ear of the mice. The left ear received acetone, delivered in the same manner. Treatments were given orally at a dose of 300 μmol/kg (suspension in arabic gum 5%) 1 h before TPA or AA application. Finally, mice were killed by ether inhalation and 7 mm diameter of right and left ears was cut and weighed. Ear edema was measured as the differences in weight between the challenged and the unchallenged ear. Percent inhibition was calculated by using $(C - T)/C \times 100$ (%), where C and T indicate non-treated (vehicle) edema and drug-treated edema, respectively. Measurements were taken 6h after TPA-induced and 1h after AA-induced ear edema.

4.2.3. Formalin-induced murine pain model.[27] The formalin-induced pain test was carried out as described by Hunskaar and Hole.[27] Animals were injected subplantarly with 20 μL of 2.5% formalin in one hind paw. The compounds were administered orally (100 μmol/kg in arabic gum 5% as vehicle) 60 min before formalin injection. The time the mice spent licking or biting the injected paw or leg was recorded. Two distinct periods of intensive licking activity were identified and scored separately unless otherwise stated. The first period (earlier or neurogenic phase) was recorded 0–5 min after formalin injection and the second period (later or inflammatory phase) was recorded 15–30 min after injection.

4.2.4. Hot plate test in mice.[28] Central analgesic activity was investigated using the hot plate test as previously described.[28] Swiss mice of both sexes (18–25 g) were used, maintained with water ad libitum, and fasted for 8 h. In these experiments, the hot plate apparatus (Ugo Basile, Model-DS 37) was maintained at 55 ± 1 °C. Mice were placed on the heated surface at 0, 30, 60, 90, and 120 min after oral administration of vehicle, morphine (39.5 μmol/kg, used as positive control) or test compounds (100 μmol/kg) and the time between placement and the first sign of paw licking or jumping was recorded as latency. The basal latencies were found to be 6–10 s. A cut-off time of 25 s was followed to prevent any injury to the paws.

4.2.5. CB1-binding profile in murine brain homogenate toward [^{3}H]SR141716A.[29] Swiss mice weighing between 30 and 40 g were used. Animals were sacrificed by decapitation, taking off the whole brain for the assay. Brains were homogenized in buffer A (320 mM sucrose, 50 mM Tris–HCl, 1 mM EDTA, and 5 mM $MgCl_2$, pH 7.4) in a glass potter (10 movements). For 4 brains, 20 mL of buffer A (5 mL to homogenize and 15 mL to rinse) was used. The homogenate was centrifuged at 5400 rpm for 10 min at 4 °C. The supernatant was saved, and the pellet washed once in 10 mL of buffer A with subsequent centrifugation. The combined supernatants were centrifuged at 21,000 rpm for 1h at 4 °C. The pellet was resuspended in 1 mL of buffer B (50 mM Tris–HCl, 1 mM EDTA, and 3 mM $MgCl_2$, pH 7.4) to yield a protein concentration of approximately 4–6 mg/mL. Binding was initiated by the addition of 160 μg membrane protein to silanized tubes containing 50 μL (10 nM) PMSF (amidase-FAAH inhibitor), 50 μL (10 nM) of [^{3}H]SR141716A, 50 μL of vehicle (0,1 % DMSO + buffer C) or 50 μL AM281, SR141716A analog (CB1 receptor antagonist, 100 μM) or testing compound and a sufficient volume of buffer

C (50 mM Tris–HCl, 1 mM EDTA, 3 mM $MgCl_2$, and 2.5 mg/mL fatty acid-free BSA, pH 7.4) to bring the total volume to 500 μL. The addition of 100 μM unlabeled AM281 was used to assess non-specific binding. Following incubation (30 °C for 1 h), binding was terminated by the addition of 1 mL of ice-cold buffer D (50 mM Tris–HCl, pH 7.4, plus 1 mg/mL BSA) to complete volume to 1.5 mL, and vacuum filtration. Filters should be pre-treated with polyethyleneimine (0.1%) for at least 2 h. Tubes were rinsed with 2 mL of ice-cold buffer D, which was also filtered, and the filters were subsequently rinsed twice with 4 mL of ice-cold buffer D. Filters were shaken for 1 h in 4 mL of scintillation fluid, before radioactivity was quantified by liquid scintillation spectrometry.

4.2.6. Cell proliferation assay.[30] Enriched T cells were obtained by nylon wool filtration of splenocytes[29] depleted of RDC by treatment with Tris-buffered ammonium chloride. Nylon wool-enriched T cells were resuspended in DMEM (Invitrogen, Life Technologies), supplemented with 2 mM glutamine, 5×10^{-5} M 2-Me, 10 μg/mL gentamicin, 1 mM sodium pyruvate, and 0.1 mM MEM non-essential amino acids plus 1% of nutridoma (Roche). Cultures (0.2 mL) were established in triplicate in 96-well flat-bottomed microtiter plates (TPP-Germany) with or without soluble anti-CD3 (2% v/v of 145.2C11 mAb), and PMA (0.5 ng/mL, Sigma) in the presence of the indicated compound. Cultures were incubated for 3 days at 37 °C in a humidified atmosphere containing 7% CO_2. The cells were pulsed with [^{3}H]thymidine (Amersham Co., UK; 1.0 μCi/well) over the last 18 h and harvested onto glass fiber filter mats. Radioactive incorporation into DNA was determined by liquid scintillation spectrometry.

4.2.7. T cell death assay.[31] Nylon wool-enriched T cells were adjusted to 10^6 cells ml^{-1} in DMEM plus 1% nutridoma, distributed in 24-well plate (1 mL, *TPP* Switzerland) and cultured with medium only or were stimulated with anti-CD3 (145.2C11 mAb) in the presence of PMA, and with or without LASSBio-881 (**3c**) or anandamide (AEA). After 48 h at 37 °C and 7% CO_2 in a humid atmosphere, cells were collected and stained with FITC-annexin V (PharMingem, BD) and 7-AAD (Calbiochem, CA) and then analyzed by flow cytometry (FACScalibur, BD).

4.3. Antioxidant assays

4.3.1. Cyclic voltammetry.[32] Electrochemical studies were carried out in dimethylformamide (DMF) containing 0.1 M tetrabutylammonium perchlorate (TBAP), using a glassy carbon electrode BAS (diameter = 3.0 mm) as a working electrode, a platinum-wire electrode as a counter electrode, and a home-built $Ag|AgCl|Cl^-$ 0.1 M NaCl Luggin reference electrode, isolated from the solution by a Vycor® rod. The scan rate v was in the range 0.010–2 V s^{-1}.

4.3.2. DPPH assay.[34] Two milliliters of an ethanolic solution of test compounds was added to 2 mL of a DPPH ethanolic solution (1×10^{-4} M) (Sigma), and the reaction mixture was vigorously shaken at ambient temperature. DPPH absorption was spectrophotometrically measured at 514 nm. Mean values were obtained from triplicates.

4.3.3. Hydroxyl-mediated deoxyribose degradation.[35] Reaction mixtures (0.5 mL) containing 2-deoxy-D-ribose (10 mM), Hepes, pH 7.2 (10 mM), test compounds (10 μL) dissolved in DMSO (0.5 mM), and H_2O_2 (1 mM) were incubated at 37 °C for 1 h. The reaction was started by addition of $Fe(NH_4)_2(SO_4)_2.6H_2O$ (10 μM). The controls were run in the absence of 2-deoxy-D-ribose. Thiobarbituric acid (1% in 50 mM NaOH, 0.5 mL) and *o*-phosphoric acid (4%, 0.5 mL) were then added and the reaction mixture was heated at 90–100 °C for 15 min and cooled, and the absorbance was determined at 532 nm (19–21). The molar extinction coefficient used to determine the thiobarbituric acid reactive substance (TBARS) concentration was $1{,}56 \times 10^5$ M^{-1} cm^{-1}.

4.3.4. Superoxide scavenging.[36] Compounds (0.25 mM) dissolved in DMSO were added to phosphate buffer (50 mM, pH 7.8, 37 °C) containing xanthine (0.25 mM), EDTA (0.10 mM), and cytochrome *c* (12 μM). Reaction was started by adding xanthine oxidase (~0.2 U/mL, in EDTA 0.1 mM). Reduction rates of cytochrome *c* by superoxide anion were measured spectrophotometrically at the Soret band and expressed as ΔA/min.

4.4. Molecular modeling

Systematic conformational analysis of NAH compound LASSBio-881 (**3c**) diastereomers was performed using semi-empirical Hamiltonian AM1 method[37] within SPARTAN 1.0.5 Pro software[38] running on Pentium IV 1.5 GHz. Lowest energy conformers for each diastereomer were used to evaluate the radical energy profile.

Acknowledgments

The authors thank CAPES (BR), CNPq (BR), FAPEAL (BR), FAPERJ (BR), FAPESP (BR), PRONEX (BR), and IM-INOFAR (BR, #420015/05-1) for financial support and fellowships (to C.D.D., J.L.M.T., D.I.L., M.V.M., F.D., E.J.H.B., F.S.P., M.O.F.G., J.B.C., A.L.P.M., C.A.M.F., E.J.B.).

References and notes

1. Nathan, C. *Nature* **2002**, *420*, 846.
2. Williams, M.; Kowaluk, E. A.; Arneric, S. P. *J. Med. Chem.* **1999**, *42*, 1481.
3. Smith, W. L.; Meade, E. A.; DeWitt, D. L. *Ann. N. Y. Acad. Sci.* **1994**, *714*, 136; Vane, J.; Bakhle, Y. S.; Botting, R. M. *Ann. Rev. Pharmacol. Toxicol.* **1998**, *38*, 97.
4. Vane, J. R.; Botting, R. M. *Inflamm. Res.* **1995**, *44*, 1.
5. Warner, T. D.; Giuliano, F.; Vojnovic, I.; Bukasa, A.; Mitchell, J. A.; Vane, J. R. *Proc. Natl. Acad. Sci. U.S.A.* **1999**, *96*, 7563.

6. Calignano, A.; La Rana, G.; Giuffrida, A.; Piomelli, D. *Nature* **1998**, *394*, 277.
7. Richardson, J. D.; Aanonsen, L.; Hargreaves, K. M. *Eur. J. Pharmacol.* **1998**, *345*, 145; Richardson, J. D.; Kilo, S.; Hargreaves, K. M. *Pain* **1998**, *75*, 111.
8. Howlett, A. C.; Barth, F.; Bonner, T. I.; Cabral, G.; Casellas, P.; Devane, W. A.; Felder, C. C.; Herkenham, M.; Mackie, K.; Martin, B. R.; Mechoulam, R.; Pertwee, R. G. *Pharmacol. Rev.* **2002**, *54*, 161.
9. Lambert, D. M.; Fowler, C. J. *J. Med. Chem.* **2005**, *48*, 5059.
10. Hampson, A. J.; Hill, W. A.; Zan, P. M.; Makriyannis, A.; Leung, E.; Eglen, R. M.; Bornheim, L. M. *Biochim. Biophys. Acta* **1995**, *1259*, 173; Kozak, K. R.; Rowlinson, S. W.; Marnett, L. J. *J. Biol. Chem.* **2000**, *275*, 33744; Veldhuis, W. B.; van der Stelt, M.; Wadman, M. W.; van Zadelhoff, G.; Maccarrone, M.; Fezza, F.; Veldink, G. A.; Vliegenthart, J. F. G.; Bar, P. R.; Nicolay, K.; Di Marzo, V. *J. Neurosci.* **2003**, *23*, 4127; Craib, S. J.; Ellington, H. C.; Pertwee, R. G.; Ross, R. A. *Br. J. Pharmacol.* **2001**, *134*, 30; van der Stelt, M.; van Kuik, J. A.; Bari, M.; van Zadelhoff, G.; Leeflang, B. R.; Veldink, G. A.; Finazzi-Agro, A.; Vliegenthart, J. F. G.; Maccarrone, M. *J. Med. Chem.* **2002**, *45*, 3709.
11. Di Virgilio, F. *Curr. Pharm. Des.* **2004**, *10*, 1647.
12. Chong, Z. Z.; Li, F. Q.; Maiese, K. *Prog. Neurobiol.* **2005**, *75*, 207.
13. Candelario-Jalil, E.; González-Falcón, A.; García-Cabrera, M.; Álvarez, D.; Al-Dalain, S.; Martínez, G.; León, O. S.; Springer, J. E. *J. Neurochem.* **2003**, *86*, 545; Candelario-Jalil, E.; León, O. S. *BMC Pharmacol.* **2003**, *3*, 7; Candelario-Jalil, E.; Alvarez, D.; González-Falcón, A.; Garcia-Cabrera, M.; Martinez-Sanchez, G.; Merino, N.; Giuliani, A.; Leon, O. S. *Eur. J. Pharmacol.* **2002**, *453*, 189.
14. For a recent review on NAH, see: (a) Fraga, C. A. M.; Barreiro, E. J. *Curr. Med. Chem.* **2006**, *13*, 167; (b) Fraga, A. G. M.; Rodrigues, C. R.; Miranda, A. L. P.; Barreiro, E. J.; Fraga, C. A. M. *Eur. J. Pharm. Sci.* **2000**, *11*, 285; (c) Figueiredo, J. M.; Câmara, C. A.; Amarante, E. G.; Miranda, A. L. P.; Santos, F. M.; Rodrigues, C. R.; Fraga, C. A. M.; Barreiro, E. J. *Bioorg. Med. Chem.* **2000**, *8*, 2243; (d) Lima, P. C.; Lima, L. M.; da-Silva, K. C. M.; Léda, P. H. O.; Miranda, A. L. P.; Fraga, C. A. M.; Barreiro, E. J. *Eur. J. Med. Chem.* **2000**, *35*, 187; Cunha, A. C.; Figueiredo, J. M.; Tributino, J. L. M.; Miranda, A. L. P.; Castro, H. C.; Zingali, R. B.; Fraga, C. A. M.; de-Souza, M. C. B. V.; Ferreira, V. F.; Barreiro, E. J. *Bioorg. Med. Chem.* **2003**, *11*, 2051; Silva, G. A.; Costa, L. M. M.; Brito, F. C. F.; Miranda, A. L. P.; Barreiro, E. J.; Fraga, C. A. M. *Bioorg. Med. Chem.* **2004**, *12*, 3149.
15. (a) Barreiro, E. J.; Fraga, C. A. M.; Miranda, A. L. P.; Rodrigues, C. R. *Quim. Nova* **2002**, *25*, 129; (b) Mahy, J. P.; Gaspard, S.; Mansuy, D. *Biochemistry* **1993**, *32*, 4014.
16. Fraga, C. A. M.; Barreiro, E. J. *Curr. Med. Chem.* **2006**, *13*, 167.
17. Barreiro, E. J.; Fraga, C. A. M. Estratégias de modificação molecular. In *Química Medicinal: as bases moleculares da ação dos fármacos*; Artmed Editora: Porto Alegre, Brazil, 2001; pp 163–210.
18. Miranda, A. L. P.; Lima, P. C.; Tributino, J. L. M.; Melo, P. A.; Fernandes, P. D.; Cintra, W. M.; Fraga, C. A. M.; Barreiro, E. J. *Abstracts du 6^{éme} Congrès Annuel de la Société Française de Pharmacologie* **2002**, P296, Rennes, France.
19. vonGadow, A.; Joubert, E.; Hansmann, C. F. *J. Agric. Food Chem.* **1997**, *45*, 632.
20. Barreiro, E. J.; Fraga, C. A. M. *Quim. Nova* **1999**, *22*, 744.
21. Barreiro, E. J.; Lima, M. E. F. *J. Pharm. Sci.* **1992**, *81*, 1219; Barreiro, E. J.; Costa, P. R. R.; Coelho, F. A. S.; De-Farias, F. M. C. *J. Chem. Res. (S)* **1985**, 220.
22. Ekeley, J. B.; Klemme, M. *J. Am. Chem. Soc.* **1928**, *50*, 2711.
23. Karabatsos, G. J.; Graham, J. D.; Vane, F. M. *J. Am. Chem. Soc.* **1962**, *84*, 753; Karabatsos, G. J.; Taller, R. A. *J. Am. Chem. Soc.* **1963**, *85*, 3624; Karabatsos, G. J.; Shapiro, B. L.; Vane, F. M.; Fleming, J. S.; Ratka, J. S. *J. Am. Chem. Soc.* **1963**, *85*, 2784.
24. Silva, A. G.; Zapata-Sudo, G.; Kummerle, A. E.; Fraga, C. A. M.; Barreiro, E. J.; Sudo, R. T. *Bioorg. Med. Chem.* **2005**, *13*, 3431.
25. Ferreira, S. H. *J. Pharm. Pharmacol.* **1979**, *31*, 648.
26. Sánchez, T.; Moreno, J. *Prostaglandins Other Lipid Mediat.* **1999**, *57*, 119; Qian, C.; Hwang, S. B.; Libertine-Garahan, L.; Eckman, J. B.; Cai, X.; Scannell, R. T.; Yeh, C. G. *Pharmacol. Res.* **2001**, *44*, 213.
27. Hunskaar, S.; Hole, K. *Pain* **1987**, *30*, 103.
28. Kuraishi, Y.; Harada, Y.; Aratani, S.; Satoh, M.; Takagi, H. *Brain Res.* **1983**, *273*, 245.
29. Abood, M. E.; Ditto, K. E.; Noel, M. A.; Showalter, V. M.; Tao, Q. *Biochem. Pharmacol.* **1997**, *53*, 207.
30. Julius, M. H.; Simpson, E.; Herzenberg, L. A. *Eur. J. Immunol.* **1973**, *10*, 645; Hirata, T.; Shimazaki, C.; Sumikuma, T.; Ashihara, E.; Goto, H.; Inaba, T.; Koishihara, Y.; Nakagawa, M. *Leuk. Res.* **2003**, *27*, 343.
31. Schmid, I.; Uittenbogaart, C. H.; Keld, B.; Giorgi, J. V. *J. Immunol. Methods* **1994**, *170*, 145.
32. Cavalcanti, J. C. M.; Oliveira, N. V.; De-Moura, M. A. B. F.; Fruttero, R.; Bertinaria, M.; Goulart, M. O. F. *J. Electroanal. Chem.* **2004**, *571*, 177.
33. Lund, H. Cathodic Reduction of Nitro and Related Compounds. In *Organic Electrochemistry*; Lund, H., Hammerich, O., Eds., 4th ed.; Marcell Dekker: NewYork, 2001; pp 379–401; Lund, H. Reduction of Azomethine Compounds. In *Organic Electrochemistry*; Lund, H., Hammerich, O., Eds., 4th ed.; Marcell Dekker: New York, 2001; pp 435–451; Morrow, G. W. Anodic Oxidation of Oxygen-Containing Compounds. In *Organic Electrochemistry*; Lund, H., Hammerich, O., Eds., 4th ed.; Marcell Dekker: New York, 2001; pp 589–620.
34. Brand-Williams, W.; Cuvelier, M. E.; Berset, C. *Lebensm.-Wiss. u.-Technol.* **1995**, *28*, 25.
35. Meinicke, A. R.; Bechara, E. J. H.; Vercesi, A. E. *Arch. Biochem. Biophys.* **1998**, *349*, 275.
36. Flohé, L.; Ötting, F. *Methods Enzymol.* **1984**, *105*, 93.
37. Dewar, M. J. S.; Zoebisch, E. G.; Healy, E. F.; Stewart, J. J. P. *J. Am. Chem. Soc.* **1985**, *107*, 3902.
38. Wavefunction Inc., Irvine, CA, 2000.
39. Zuman, P.; Fijalek, Z. *J. Electroanal. Chem.* **1990**, *296*, 583.